

Aqua Ions. 1. The Structures of the $[\text{Ru}(\text{OH}_2)_6]^{3+}$ and $[\text{V}(\text{OH}_2)_6]^{3+}$ Cations in Aqueous Solution: An EPR and UV–Vis Study

Stefan Dolder, David Spichiger, and Philip L. W. Tregenna-Piggott*

Department of Chemistry and Biochemistry, University of Bern, Freiestrasse 3, CH-3000, Bern 9, Switzerland

Received August 21, 2002

Spectroscopic data are presented for the $[\text{V}(\text{OH}_2)_6]^{3+}$ and $[\text{Ru}(\text{OH}_2)_6]^{3+}$ cations, from which inferences are drawn regarding their structures in aqueous solution. EPR and absorption spectra of solutions and glasses are supplemented by spectra of the aqua ions in various crystalline environments, and the electronic and molecular structures inter-related through elementary angular overlap model calculations. It is concluded that in aqueous solution the $[\text{Ru}(\text{OH}_2)_6]^{3+}$ cation is localized in the all-horizontal D_{3d} geometry, whereas the structure of the $[\text{V}(\text{OH}_2)_6]^{3+}$ cation is close to T_h symmetry. These results are consistent with the most energetically favored geometries predicted by ab initio calculations.

1. Introduction

The interplay between the molecular and electronic structure of transition metal complexes is of key importance to understanding their physical and chemical properties. Many model studies have focused on the aqua ions,^{1–9} due to their ubiquity, and the singular nature of the metal–water interaction.^{8,9} The most symmetrical arrangement of six water ligands about the metal center gives rise to T_h symmetry (Figure 1), which is predicted to be favored by complexes with nondegenerate ground terms.³ For complexes with orbital doublet ground terms, such as Cr(II) and Mn(III), a pronounced, classical Jahn–Teller distortion is anticipated, involving a tetragonal elongation of the $\text{M}^{\text{III}}\text{O}_6$ framework;³ and numerous examples have been cited.^{10–12} The optimal

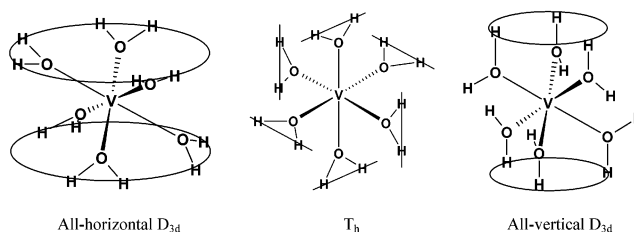


Figure 1. Possible high-symmetry structures of the $[\text{V}(\text{OH}_2)_6]^{3+}$ cation. The structures are distinguished by the value of the twist angle, φ , defined in the caption of Figure 2. For the all-horizontal D_{3d} , T_h , and all-vertical D_{3d} geometries shown, $\varphi = -45^\circ$, 0° , and $+45^\circ$ respectively.

hydration structure favored by complexes with orbital triplet ground terms is a more contentious issue.^{1–4,13–16} The t_{2g} (O_h) orbitals are weakly π -antibonding; and their energies are most sensitive to a concerted rotation of the water ligands about the M–O bond vectors,² leading to the all-horizontal (e_g component lower lying) or all-vertical (a_g component lower lying) D_{3d} geometries (Figure 1).¹⁴ For second- and third-row transition metal aqua ions with orbital triplet

* Corresponding author. E-mail: tregenna@iac.unibe.ch.

- (1) Tachikawa, H.; Ichikawa, T.; Yoshida, H. *J. Am. Chem. Soc.* **1990**, *112*, 977–982.
- (2) Tachikawa, H.; Ichikawa, T.; Yoshida, H. *J. Am. Chem. Soc.* **1990**, *112*, 982–987.
- (3) Åkesson, R.; Pettersson, L. G. M.; Sandström, M.; Wahlgren, U. *J. Am. Chem. Soc.* **1994**, *116*, 8691–8704.
- (4) Kallies, B.; Meier, R. *Inorg. Chem.* **2001**, *40*, 3101.
- (5) Hartmann, M.; Clark, T.; Van Eldik, R. *J. Phys. Chem. A* **1999**, *103*, 9899–9905.
- (6) Tregenna-Piggott, P. L. W.; Best, S. P.; O'Brien, M. C. M.; Knight, K. S.; Forsyth, J. B.; Pilbrow, J. R. *J. Am. Chem. Soc.* **1997**, *119*, 3324–3332.
- (7) Hitchman, M. A.; Maaskant, W.; Van der Plas, J.; Simmons, C. J.; Stratemeier, H. *J. Am. Chem. Soc.* **1999**, *121*, 1488–1501.
- (8) Best, S. P.; Figgis, B. N.; Forsyth, J. B.; Reynolds, P. A.; Tregenna-Piggott, P. L. W. *Inorg. Chem.* **1995**, *34*, 4605–4610.
- (9) Fender, B. E. F.; Figgis, B. N.; Forsyth, J. B.; Reynolds, P. A.; Stevens, E. *Proc. R. Soc. London, Ser. A* **1986**, *404*, 127–138.

- (10) Telser, J.; Pardi, L. A.; Krzystek, J.; Brunel, L.-C. *Inorg. Chem.* **1998**, *37*, 5769.
- (11) Riley, M. J. *Top. Curr. Chem.* **2001**, *214*, 57.
- (12) Tregenna-Piggott, P. L. W.; Andres, H.-P.; McIntyre, G. J.; Best, S. P.; Wilson, C. C.; Cowan, J. A. *Inorg. Chem.* **2003**, *42*, 1350–1365.
- (13) Cotton, F. A.; Fair, C. K.; Lewis, G. E.; Mott, G.; Moss, F. K.; Schultz, A. J.; Williams, M. J. *J. Am. Chem. Soc.* **1984**, *106*, 5319.
- (14) Best, S. P.; Forsyth, J. B. *J. Chem. Soc., Dalton Trans.* **1991**, 1721.
- (15) Beattie, J. K.; Best, S. P.; Del Favero, P.; Skelton, B. W.; Sobolev, A. N.; White, A. H. *J. Chem. Soc., Dalton Trans.* **1996**, 1481.
- (16) Tregenna-Piggott, P. L. W.; Best, S. P.; Güdel, H. U.; Weihe, H.; Wilson, C. C. *J. Solid State Chem.* **1999**, *145*, 460.

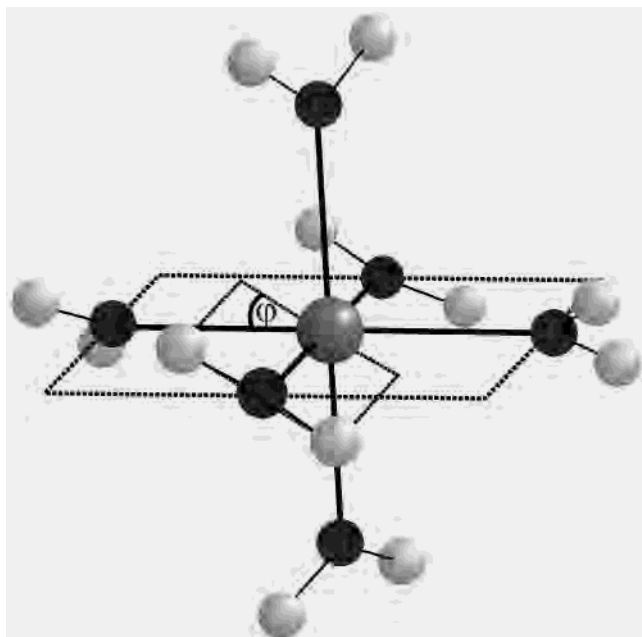


Figure 2. Definition of the twist angle, φ , characterizing the mode of water coordination in a hexaqua complex. φ denotes the degree by which the H_2O plane is rotated about the $\text{M}-\text{O}$ bond vector and is formally defined as the angle between the horizontal plane (defined with the 3-fold axis running through the top front octant of the MO_6 octahedron) and the plane which contains the $\text{M}-\text{O}$ bond vector and is parallel to the $\text{H}-\text{H}$ bond vector of the coordinated water molecule. φ is $\sim -20^\circ$ for the complex shown in the figure.

ground terms, *ab initio* calculations predict the energy minima to be strongly localized in either of the D_{3d} geometries;² whereas for the corresponding first-row transition metal aqua ions, such as $[\text{Ti}(\text{OH}_2)_6]^{3+}$ and $[\text{V}(\text{OH}_2)_6]^{3+}$, the tendency to distort is tempered, to a greater degree, by steric effects.⁴ DFT calculations by Kallies and Meier suggest that the calculated $T_h-S_6-D_{3d}$ potential energy surface is rather shallow for the $[\text{V}(\text{OH}_2)_6]^{3+}$ and $[\text{Ti}(\text{OH}_2)_6]^{3+}$ cations.⁴ With the orientation of the plane of the water molecule, with respect to a regular MO_6 framework, defined by the twist angle, φ ,¹⁴ depicted in Figure 2, $\varphi = 0^\circ$ for T_h symmetry and $\varphi = 45^\circ$ and -45° for the all-vertical and all-horizontal D_{3d} structures, respectively. For intermediate values of φ , the aqua ion possesses S_6 (C_{3i}) point symmetry, and the theoretical minima for $[\text{V}(\text{OH}_2)_6]^{3+}$ and $[\text{Ti}(\text{OH}_2)_6]^{3+}$ are found at $\varphi = -9.4^\circ$ and 13.6° respectively.⁴

The array of theoretical calculations reported for aqua ions are all performed on discrete molecular units at 0 K in the gas phase.¹⁻⁴ Therefore, while potentially instructive, the relevance of these calculations to chemistry is questionable, and many of the theoretical predictions await any kind of experimental support. The structure of the $[\text{Ti}(\text{OH}_2)_6]^{3+}$ cation in an amorphous solid of a 2-propanol/ D_2O mixture was determined to be close to all-vertical D_{3d} ,¹ whereas the $[\text{V}(\text{OH}_2)_6]^{3+}$ cation adopts the all-horizontal D_{3d} geometry in the triflate salt $[\text{V}(\text{OH}_2)_6][\text{H}_5\text{O}_2](\text{CF}_3\text{SO}_3)_4$.¹³ These results are at variance with the calculations of Kallies and Meier, although such discrepancies can always be imputed to hydrogen-bonding constraints.⁴

This work presents an experimental study of the electronic structures of the $[\text{V}(\text{OH}_2)_6]^{3+}$ and $[\text{Ru}(\text{OH}_2)_6]^{3+}$ cations in

aqueous solution, from which inferences are drawn regarding their geometries. Our conclusions do indeed tally with the most energetically favored structures predicted by theory.

The experimental data which we shall describe provide information on the magnitude of the axial field splitting of the ${}^2T_{2g}$ (O_h) and ${}^3T_{1g}$ (O_h) ground terms of the $[\text{Ru}(\text{OH}_2)_6]^{3+}$ and $[\text{V}(\text{OH}_2)_6]^{3+}$ cations, respectively. The wealth of experimental and theoretical work on aqua ions, with orbital triplet ground terms, has shown that the orbital components of the ground term are most sensitive to displacements along the twisting internal coordinate, as defined by the twist angle φ .^{2,4,14,17} The relationship between the trigonal field splitting of the ground term, and a concomitant rotation of the water molecules about the $\text{M}-\text{O}$ bond vectors, in the formalism of the angular overlap model (AOM), is given by^{14,17}

$$\Delta = 3(e_{\pi\perp} - e_{\pi\parallel}) \sin(2\varphi) \quad (1)$$

where $e_{\pi\perp}$ and $e_{\pi\parallel}$ parametrize the π -bonding normal to and in the plane of the water molecule, respectively. When Δ is negative, the e_g component of the t_{2g} one-electron orbitals is lower lying, yielding nondegenerate trigonal ground terms for the Ru(III) and V(III) hexaqua cations. Using this simple expression, excellent agreement has been obtained between the value of φ , determined from crystallography, and the energy of the ${}^3A_g \rightarrow {}^3E_g$ (S_6) electronic Raman transition of the $[\text{V}(\text{OH}_2)_6]^{3+}$ cation, in a variety of crystal systems.¹⁸⁻²⁰ This expression is employed to relate the electronic and molecular structures of the $[\text{V}(\text{OH}_2)_6]^{3+}$ and $[\text{Ru}(\text{OH}_2)_6]^{3+}$ cations in aqueous solution.

For both the $[\text{V}(\text{OH}_2)_6]^{3+}$ and $[\text{Ru}(\text{OH}_2)_6]^{3+}$ cations, the data obtained in aqueous media are complemented by studies of the aqua ions in various crystal systems, where the structures are, in part, dictated by hydrogen-bonding constraints, and the values of φ have been determined by crystallography. Solid-state data are presented, or discussed, for double sulfate salts of general formula $\text{M}^I[\text{M}^{III}(\text{OH}_2)_6](\text{SO}_4)_2 \cdot \text{XH}_2\text{O}$, where the structural modification can be altered by changing either the monovalent or trivalent cation.^{15,21-23} In the β -alum modification, the trivalent cation lies on a site of S_6 symmetry, the mode of water coordination is trigonal planar, and values of φ in the range -19.0° to -22.0° have been determined, depending on the identity of the trivalent cation.^{12,14} In the α -alums, the site symmetry is also S_6 , but the value of φ is now $\sim 0^\circ$, and the angle between the $\text{M}-\text{O}$ bond vector and the water plane is $\sim 19^\circ$.²⁴ Such a tilt of the water molecules is predicted to reduce slightly the magnitude of the metal-water π anisotropy,

(17) Daul, C.; Goursot, A. *Inorg. Chem.* **1985**, *24*, 3554-3558.

(18) Best, S. P.; Clark, R. J. H. *Chem. Phys. Lett.* **1985**, *122*, 401.

(19) Tregenna-Piggott, P. L. W.; Best, S. P. *Inorg. Chem.* **1996**, *35*, 5730.

(20) Spichiger, D.; Carver, G.; Dobe, C.; Bendix, J.; Tregenna-Piggott, P. L. W.; Meier, R.; Zahn, G. *Chem. Phys. Lett.* **2001**, *337*, 391.

(21) Beattie, J. K.; Best, S. P.; Skelton, B. W.; White, A. H. *J. Chem. Soc., Dalton Trans.* **1981**, 2105.

(22) Armstrong, R. S.; Beattie, J. K.; Best, S. P.; Skelton, B. W.; White, A. H. *J. Chem. Soc., Dalton Trans.* **1983**, 1973.

(23) Haussühl, S. Z. *Kristallogr., Kristallgeom., Kristallphys., Kristallchem.* **1961**, *116*, 371-405.

(24) Best, S. P.; Forsyth, J. B. *J. Chem. Soc., Dalton Trans.* **1990**, 395.

given by the quantity $(e_{\pi\perp} - e_{\pi\parallel})$.²⁵ When the identity of the monovalent cation is changed from a group I metal to the guanidinium cation, [C(NH₂)₃]⁺, the space group changes from cubic (*Pa*3) to trigonal (*P*31*m*).²⁰ In the guanidinium salts there are two crystallographically distinct sites for the aqua ion to occupy, one of *C*₃ symmetry, the other *C*_{3*v*}, present in the ratio 2:1. The stereochemistry of the [V(OH₂)₆]³⁺ cation in the guanidinium salt differs little for the two sites, with $\varphi \sim -45^\circ$, and an average tilt of the water molecules of $\sim 9^\circ$.²⁰ For the studies in aqueous media, solutions were prepared with either trifluoromethanesulfonate (triflate) or *p*-toluenesulfonate, as the counterion. These anions are known to be very poor ligands, and are not expected to displace water from the first coordination sphere of the aqua complex.

Throughout this work a number of abbreviations are employed, examples of which are M^IVSH = M^I[V(OH₂)₆](SO₄)₂·XH₂O; M^I[Ga:Ru]SH = Ru(III)-doped M^IGaSH; [Ru(OH₂)₆]³⁺:trif = [Ru(OH₂)₆]³⁺ in a dilute triflic acid/glycerol glass; [Ru(OH₂)₆]³⁺:tos = [Ru(OH₂)₆]³⁺ in a dilute *p*-toluenesulfonic acid/glycerol glass.

2. Experimental Section

Synthesis. [Ru(OH₂)₆]³⁺ solutions were prepared by dissolution of [Ru(OH₂)₆](tos)₂²⁶ in *p*-toluenesulfonic acid (1 M), trifluoromethanesulfonic (triflic) acid (1 M), or sulfuric acid (1 M), to give pink solutions of Ru(II) (ca. 0.2 M). The solutions were left standing overnight, during which time the color evolved to yellow, indicative of the oxidation of [Ru(OH₂)₆]²⁺ to [Ru(OH₂)₆]³⁺.²⁷ Glycerol was applied ($\sim 50\%$ v/v) to the Ru(III) solutions prepared in *p*-toluenesulfonic and triflic acid, and the resulting mixtures were sealed under a He atmosphere in standard EPR tubes. The solution of [Ru(OH₂)₆]³⁺ in sulfuric acid was used in the preparation of Gu[Ga:Ru]SH.

Crystals of Gu[Ga:Ru]SH were prepared by addition of the solution containing [Ru(OH₂)₆]³⁺ in H₂SO₄ (1 M) to a freshly prepared saturated solution of GuGaSH (0.543 M) in H₂SO₄ (6 M). The amount of Ru(III) was estimated at ca. 1% of the total trivalent cation concentration. Crystals formed at room temperature over several days.

[V(OH₂)₆]³⁺ solutions (0.2 M) were prepared by dissolution of V(CF₃SO₃)₃ in dilute triflic acid (0.1 M) purged with argon. V(CF₃SO₃)₃ was prepared by reflux of VCl₃ (3 g) in neat triflic acid (10 g) under an argon atmosphere until HCl gas ceased to be evolved (ca. 3 h). The solution was allowed to cool to room temperature and the green precipitate of V(CF₃SO₃)₃ collected in good yield (ca. 2.5 g). The preparation of guanidinium vanadium sulfate hexahydrate (GuVSH) has been described previously.²⁰

Instrumental Details. X-band EPR spectra were recorded on a Bruker ELEXSYS spectrometer at the Department of Chemistry, University of Bern, in conjunction with an Oxford instruments ESR 910 cryostat, together with a Bruker ER 4116 DM resonator.

EPR spectra were also obtained using the high-field, multifrequency EPR facility at the CNRS, Grenoble, France. Excitation frequencies ranging from 95 to 460 GHz were employed in conjunction with a static field ranging from 0 to 12 T. The experimental setup has been described previously.²⁸

(25) Riesen H.; Dubicki, L. *Inorg. Chem.* **2000**, *39*, 2206.

(26) Bernhard, P.; Biner, M.; Ludi, A. *Polyhedron* **1990**, *9*, 1095–1097.

(27) Best, S. P.; Forsyth, J. B. *J. Chem. Soc., Dalton Trans.* **1990**, 3507.

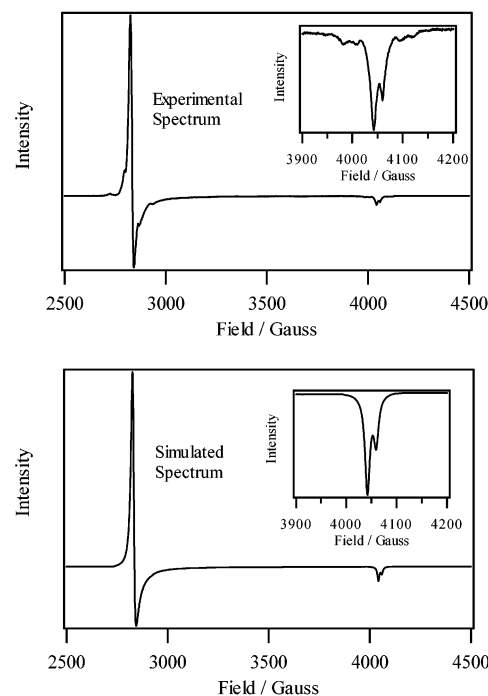


Figure 3. Experimental and simulated X-band EPR spectrum of Gu[Ga:Ru]SH. The experimental spectrum was collected at 5.0(1) K with 6.33 μ W of 9.61277 GHz radiation, and a modulation amplitude of 1 G. The simulated spectrum is a superposition of two spectra, each corresponding to an $S = 1/2$ spin system with $g_{\perp} = 2.4270$, $g_{\parallel} = 1.6990$ and $g_{\perp} = 2.4270$, $g_{\parallel} = 1.6917$ with the intensities scaled with a 2:1 ratio, respectively.

A Cary 5e spectrometer was used to collect UV–vis spectra. Polished crystals of RbVSH, GuVSH, and Rb[Ga:V]SH were sealed in a copper cell under a He atmosphere, and spectra acquired as a function of temperature. The spectrum of a freshly prepared solution of [V(OH₂)₆]³⁺ (0.2 M) in dilute triflic acid (0.1 M) was obtained using standard solution cells.

3. Results

[Ru(OH₂)₆]³⁺. In Figure 3 is shown the 5 K powder EPR spectrum of Gu[Ga:Ru]SH. The general form of the spectrum is typical for an axially symmetric $S = 1/2$ spin system with $g_{\perp} > g_{\parallel}$.²⁹ The low-field resonance, corresponding to the “z” transition, displays two peaks, with a 2:1 ratio of integrated peak intensities. The more intense band is assigned to a resonance arising from the Ru(III) cation occupying the *C*₃ site of the crystal, and the less intense band to the occupation of the *C*_{3*v*} site, in accordance with the 2:1 ratio of the sites in the crystal lattice.²⁰ The “xy” peak displays fine structure attributable to hyperfine coupling with the ⁹⁹Ru (spin $3/2$ abundance 13%) and ¹⁰¹Ru (spin $5/2$ abundance 17%) nuclei. Also shown in Figure 3 is a simulation of the spectrum, calculated using the software of Høgni Weihe.³⁰ The simulated spectrum consists of a superposition of two $S =$

(28) Muller, F.; Hopkins, A.; Coron, N.; Grynberg, M.; Brunel, L. C.; Martinez, G. *Rev. Sci. Instrum.* **1989**, *60*, 3681. Barra, A.-L.; Brunel, L. C.; Robert, J. B. *Chem. Phys. Lett.* **1990**, *165*, 107.

(29) Mabbs, F. E.; Collison, D. *Electron Paramagnetic Resonance of d Transition Metal Compounds*; Elsevier: Amsterdam, 1992.

(30) SIM, by Høgni Weihe, Department of Chemistry, University of Copenhagen. Glerup, J.; Weihe, H. *Acta Chem. Scand.* **1991**, *45*, 444–448.

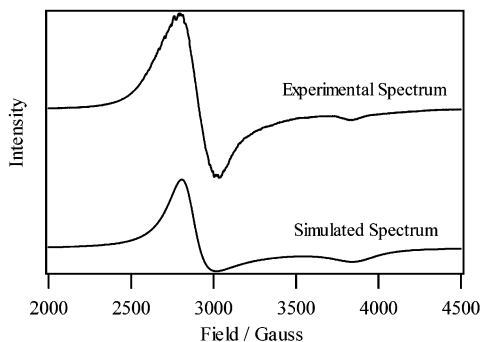


Figure 4. Experimental and simulated X-band EPR spectrum of $[\text{Ru}(\text{OH}_2)_6]^{3+}:\text{trif}$. The experimental spectrum was collected at 6.0(1) K with 0.2002 mW of 9.61296 GHz radiation, and a modulation amplitude of 4 G. The simulated spectrum corresponds to an $S = 1/2$ spin system with g values $g_{\perp} = 2.41$, $g_{\parallel} = 1.78$.

Table 1. Experimental g Values for the $[\text{Ru}(\text{OH}_2)_6]^{3+}$ Cation^a

sample	temp/K	g_{\parallel}	g_{\perp}
$[\text{Ru}(\text{OH}_2)_6]^{3+}:\text{trif}$	6	1.78(1)	2.41(2)
$[\text{Ru}(\text{OH}_2)_6]^{3+}:\text{trif}$	296	1.85(2)	2.31(2)
$[\text{Ru}(\text{OH}_2)_6]^{3+}:\text{tos}$	5	1.78(1)	2.41(2)
$[\text{Ru}(\text{OH}_2)_6]^{3+}:\text{tos}$	296	1.85(2)	2.31(2)
Cs[Ga:Ru]SH	3	1.494(5)	2.517(5)
Gu[Ga:Ru]SH (C_{3v})	5	1.6917(5)	2.427(2)
Gu[Ga:Ru]SH (C_3)	5	1.6990(5)	2.427(2)
Gu[Ga:Ru]SH	50	1.707(2)	2.422(2)
Gu[Ga:Ru]SH	296	1.76(3)	2.39(2)

^a The g values for Cs[Ga:Ru]SH were taken from ref 34.

$1/2$ spectra calculated with the g values $g_{\perp} = 2.4270$, $g_{\parallel} = 1.6990$ and $g_{\perp} = 2.4270$, $g_{\parallel} = 1.6917$ and scaled with a 2:1 ratio, respectively. Excellent agreement between theory and experiment is obtained; the hyperfine interaction was not included in the simulation.

In Figure 4 is shown the 5 K EPR spectrum of $[\text{Ru}(\text{OH}_2)_6]^{3+}:\text{trif}$. Once again the spectrum is consistent with an axially symmetric $S = 1/2$ spin system with $g_{\perp} > g_{\parallel}$, suggesting that, in solution, the $[\text{Ru}(\text{OH}_2)_6]^{3+}$ cation adopts a geometry of approximate axial symmetry. Also shown in Figure 4 is a spectral simulation calculated with $g_{\perp} = 2.41$, $g_{\parallel} = 1.78$, giving reasonable agreement with experiment. The EPR spectrum of $[\text{Ru}(\text{OH}_2)_6]^{3+}:\text{tos}$ was virtually identical.

The EPR spectrum of the $[\text{Ru}(\text{OH}_2)_6]^{3+}$ cation could be monitored up to room temperature for the crystalline and glassy samples. In all cases the g values converged as the samples were warmed. A distinct axial spectrum could still be observed for the glassy samples at 295 K, suggesting that, at this temperature, the rate of reorientation of the $[\text{Ru}(\text{OH}_2)_6]^{3+}$ cation is slow on the EPR time scale. A compilation of g values vs temperature is given in Table 1.

$[\text{V}(\text{OH}_2)_6]^{3+}$. The room temperature absorption spectrum of $[\text{V}(\text{OH}_2)_6]^{3+}$ (0.2 M) in dilute triflic acid (0.1 M) is shown in Figure 5. The spectrum is characterized by two broad bands, assigned to the ${}^3T_{1g}(\text{F}) \rightarrow {}^3T_{2g}(\text{F})$ and ${}^3T_{1g}(\text{F}) \rightarrow {}^3T_{1g}(\text{P})$ (O_h) ligand field transitions, depicted in Figure 6. Band maxima are found at 16 800 (595 nm) and 25 000 cm^{-1} (400 nm). In addition, a weak band at ca. 13 000 cm^{-1} (770 nm) is visible in the spectrum. The position of the band is coincident with that expected for the vanadyl ion,³¹ and a gain in intensity was observed after oxygen was bubbled

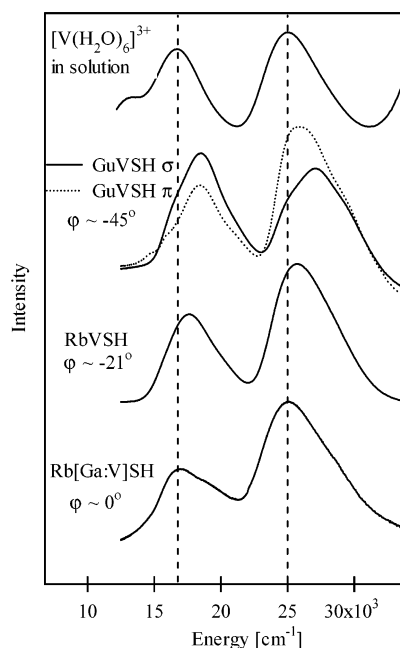


Figure 5. Room temperature electronic spectra of the $[\text{V}(\text{OH}_2)_6]^{3+}$ cation, in a dilute triflic acid solution, and in three different crystal systems.

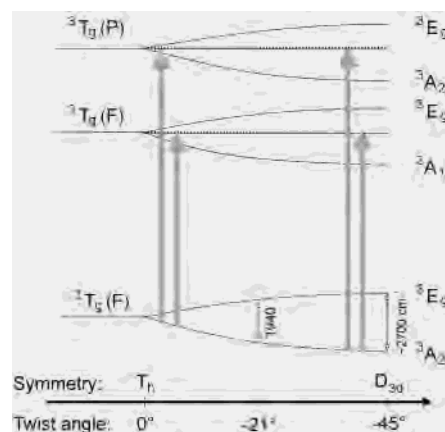


Figure 6. Schematic diagram depicting the expected increase in energy of the ${}^3T_{1g}(\text{F}) \rightarrow {}^3T_{2g}(\text{F})$ and ${}^3T_{1g}(\text{F}) \rightarrow {}^3T_{1g}(\text{P})$ (O_h) ligand field transitions, as the twist angle decreases from 0° (T_h symmetry) to -45° (all-horizontal D_{3d} symmetry). The broken lines denote the center-of-gravity of the ${}^3T_{2g}(\text{F})$ and ${}^3T_{1g}(\text{P})$ terms. The values of the trigonal field splitting of ${}^3T_{1g}(\text{F})$ ground term, shown on the figure, were determined by electronic Raman spectroscopy.

through the solution for a 10 min period. The weak band at ca. 13 000 cm^{-1} is therefore assigned to a vanadium(IV) impurity.

Also shown in Figure 5 are room temperature absorption spectra of the $[\text{V}(\text{OH}_2)_6]^{3+}$ cation in three crystal systems, where the stereochemistries of the $[\text{V}(\text{OH}_2)_6]^{3+}$ cations, imposed by hydrogen-bonding constraints, differ primarily in the values of the twist angle φ , shown on the figure. Spectra of the cubic RbVSH (β -modification) and Rb[Ga:V]SH (α -modification) crystals were collected with unpolarized radiation. GuVSH crystallizes in the trigonal space group $P31m$. Spectra for this salt were collected with the electric vector of the incident radiation polarized parallel (π)

(31) Lever, A. B. P. *Inorganic Electronic Spectroscopy*; Elsevier: Amsterdam, 1984.

and perpendicular (σ) to the unique 3-fold axis. The low-temperature absorption spectra of [V(OH₂)₆]³⁺ in all three crystal systems have been discussed, and assigned previously.^{16,32} The room temperature spectra presented in Figure 5 differ only in that the absorption bands are broader, and are shifted slightly to lower energy. It is seen from Figure 5 that as the magnitude of φ decreases, the general shift of the ligand field bands is to lower energy. The electronic absorption bands of Rb[Ga:V]SH occur at similar energies to those observed for [V(OH₂)₆]³⁺ in aqueous solution.

An attempt was also made to obtain high-field, high-frequency EPR spectra of the [V(OH₂)₆]³⁺ cation. Good quality spectra were obtained for RbVSH and GuVSH, the data for RbVSH having been presented and interpreted previously.¹⁶ However, no signal was obtained for Rb[Ga:V]SH or for [V(OH₂)₆]³⁺:trif. The failure to observe EPR spectra in these systems cannot be attributed to the concentration of vanadium, as high-quality high-field multifrequency EPR spectra have previously been reported for Cs[Ga:V]SH recorded under the same conditions.³³

4. Discussion

[Ru(OH₂)₆]³⁺. In order to relate the experimentally determined g values of [Ru(OH₂)₆]³⁺:trif to a given stereochemistry of the complex, we must first calculate how the g values vary as a function of φ . The [Ru(OH₂)₆]³⁺ cation is a low-spin d⁵ complex, resulting in a ²T_g (T_h) ground term. Excited-state configurations are sufficiently high in energy that their influence may be neglected. It is then a straightforward task to formulate closed-form expressions for the ground-state g values of the [Ru(OH₂)₆]³⁺ cation, in terms of the spin-orbit coupling parameter, ζ , the orbital reduction factor, k , and the axial ligand field splitting, Δ , and these are given in ref 17. The first step in the analysis is then to obtain appropriate values of ζ , k , and $(e_{\pi\perp} - e_{\pi\parallel})$, which pertain to the Ru(III)-water interaction. Reports of EPR studies of the [Ru(OH₂)₆]³⁺ cation are, to our knowledge, confined to powder and single-crystal measurements on Cs[Ga:Ru]SH.³⁴ From this study, the following g values were determined at 3 K, $g_{\parallel} = 1.494(5)$, $g_{\perp} = 2.517(5)$, which were subsequently interpreted, without a knowledge of the structure.¹⁷ Following this study, neutron structures of CsGaSH¹² and CsRuSH^{27,35} have revealed regular M^{III}O₆ frameworks, trigonal planar water coordination to the trivalent cations, and values of φ equal to -19.0° and -22.0° for [Ga(OH₂)₆]³⁺ and [Ru(OH₂)₆]³⁺, respectively. Previous studies on doped alums suggest that the dopant cation largely dictates its immediate environment.¹⁶ A value of $\varphi = -22.0^\circ$ for Cs[Ga:Ru]SH is therefore assumed. Inserting eq 1 into the expressions for the ground-state g values, we calculate $g_{\parallel} = 1.494$, $g_{\perp} = 2.518$ for the following parameters: $\varphi = -22.0^\circ$, $\zeta = 980 \text{ cm}^{-1}$, $k = 0.865$, and $(e_{\pi\perp} - e_{\pi\parallel}) = 1200 \text{ cm}^{-1}$.

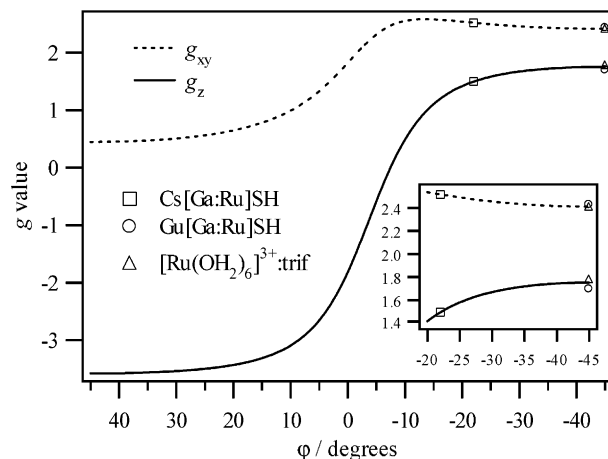


Figure 7. Theoretical and experimental g values of the [Ru(OH₂)₆]³⁺ cation. The theoretical values of g_z and g_{xy} , shown as solid and broken lines, were calculated using eq 1 and the expressions given in ref 17, with the following parameters: $(e_{\pi\perp} - e_{\pi\parallel}) = 1200 \text{ cm}^{-1}$, $\zeta = 980 \text{ cm}^{-1}$, $k = 0.865$. The squares and circles denote the principal g values determined for the Cs[Ga:Ru]SH and Gu[Ga:Ru]SH systems, respectively, with the corresponding values of φ determined from crystallography. The triangles denote the principal g values of [Ru(OH₂)₆]³⁺:trif. In this instance, the g values were plotted against $\varphi = -45^\circ$, as this gave the best agreement with the theoretical values.

The values of φ and $(e_{\pi\perp} - e_{\pi\parallel})$ equate to a trigonal field splitting, Δ , of -2500 cm^{-1} (eq 1), which compares to -1940 cm^{-1} for [V(OH₂)₆]³⁺, in the same crystal environment.¹⁹ An increase in $(e_{\pi\perp} - e_{\pi\parallel})$ is typical of the change in the ligand field parameters that occurs on substituting a first-row for a second-row transition metal element.³¹

It should be mentioned that the estimated values of ζ , k , and Δ are very similar to those proffered by Daul and Goursot, who analyzed the g values without any structural information, relying instead on results from multiple scattering X α MO calculations.¹⁷

In Figure 7 are shown the dependencies of g_{\parallel} and g_{\perp} on the angle φ , calculated using the foregoing parameters. It is seen that the principal g values are predicted to be rather sensitive to the value of φ , owing to the change in the trigonal field. We have recently published a paper on the variation of the ground-state g values of the [Ti(OH₂)₆]³⁺ cation, for values of φ between 0° and -45° .³⁶ In that work it is shown that this variation is a consequence of the change in the magnitude of the linear Jahn-Teller coupling coefficients, rather than a change in the trigonal field. Such considerations do not apply for the [Ru(OH₂)₆]³⁺ cation, as the spin-orbit coupling is so large that effects of vibronic coupling are quenched. Nevertheless, before discussing the data for [Ru(OH₂)₆]³⁺:trif, it is necessary to demonstrate that the g_{\parallel} , g_{\perp} vs φ relationships in Figure 7 provide an accurate description of the ground-state magnetic properties of the [Ru(OH₂)₆]³⁺ cation, in other coordination environments. It was with this mind that the EPR study of the Gu[Ga:Ru]SH system was undertaken, for which $\varphi \sim -45^\circ$. The principal g values for Gu[Ga:Ru]SH are shown as circles on Figure 7 and are close to the theoretical values. The experimental value of g_z

(32) Walker, I. M.; Carlin, R. L. *J. Chem. Phys.* **1967**, *46*, 3931-3936.

(33) Tregenna-Piggott, P. L. W.; Weihe, H.; Bendix, J.; Barra, A.-L.; Güdel, H.-U. *Inorg. Chem.* **1999**, *38*, 5928.

(34) Bernhard, P.; Stebler, A.; Ludi, A. *Inorg. Chem.* **1984**, *23*, 2151-2155.

(35) Best, S. P.; Forsyth, J. B.; Tregenna-Piggott, P. L. W. *J. Chem. Soc., Dalton Trans.* **1993**, 2711.

(36) Carver, G.; Bendix, J.; Tregenna-Piggott, P. L. W. *Chem. Phys.* **2002**, *282*, 245.

is slightly less than predicted, which could be a consequence of the mode of water coordination in Gu[Ga:Ru]SH being not exactly trigonal planar, as in Cs[Ga:Ru]SH.

The EPR spectrum of $[\text{Ru}(\text{OH}_2)_6]^{3+}:\text{trif}$ is characterized by well-defined g values, these being $g_{\parallel} = 1.78(1)$; $g_{\perp} = 2.41(2)$ (6 K). If the $[\text{Ru}(\text{OH}_2)_6]^{3+}$ cation were to exhibit no geometric preference in aqueous solution, adopting all possible values of φ , then this would manifest in a very wide range of possible g values, as suggested by the relationships in Figure 7. The inhomogeneous broadening would be so acute that one would not expect to observe an EPR spectrum. Instead the $[\text{Ru}(\text{OH}_2)_6]^{3+}:\text{trif}$ system has well-defined g values, which can be associated with a well-defined structure. The experimental g values of $[\text{Ru}(\text{OH}_2)_6]^{3+}:\text{trif}$ are depicted by triangles on Figure 7, and match the theoretical values for $\varphi \sim -45^\circ$, although, as the reader will observe, the theoretical g values are relatively insensitive to the value of φ in the range -35° to -45° . It is concluded that in aqueous solution the $[\text{Ru}(\text{OH}_2)_6]^{3+}$ cation adopts a geometry close to all-horizontal D_{3d} .

The g values of both Gu[Ga:Ru]SH and $[\text{Ru}(\text{OH}_2)_6]^{3+}:\text{trif}$ converge as the temperature increases (Table 1). We have recently collected single-crystal Raman data on GuGaSH, which provide no intimation of any gross structural change in this temperature range.³⁷ For the Gu[Ga:Ru]SH sample, therefore, the temperature dependence of the g values is attributed to a change in the quantity $(e_{\pi\perp} - e_{\pi\parallel})$ and/or in the quantity ζ , most likely arising from the increase in the average Ru–O bond length, which is to be expected upon increasing temperature. This being the case, the convergence of the g values of $[\text{Ru}(\text{OH}_2)_6]^{3+}:\text{trif}$ does not necessarily imply a change in the value of φ , with which we are concerned.

$[\text{V}(\text{OH}_2)_6]^{3+}$. The low-temperature, electronic absorption band profiles of GuVSH are broad but structured, and have been discussed and assigned previously, in the framework of a ligand field model.³² We have nothing further to add concerning these assignments, except to say that they should not be taken too literally. The deconvolution of the ${}^3\text{T}_{1g}(\text{F}) \rightarrow {}^3\text{T}_{2g}(\text{F})$ and ${}^3\text{T}_{1g}(\text{F}) \rightarrow {}^3\text{T}_{1g}(\text{P}) (O_h)$ spin-allowed ligand field bands into components arising from the axial field splittings of the ${}^3\text{T}_{2g}(\text{F})$ and ${}^3\text{T}_{1g}(\text{P}) (O_h)$ terms is confounded by strong excited-state Jahn–Teller effects, a very clear example of which has recently been demonstrated in the spectrum of the $[\text{VCl}_2(\text{OH}_2)_4]^+$ cation.³⁸ In an analysis of the low-temperature absorption band profiles of RbVSH and Rb[Ga:V]SH,¹⁶ we have shown that excited-state Jahn–Teller effects will tend to complicate and broaden the aforesaid ligand field transitions, beyond that expected from a simple ligand field model; and this is most clearly seen in the spectrum of Rb[Ga:V]SH, for which $\varphi \sim 0^\circ$. However, although it is true that a proper analysis of the band profiles requires a rigorous treatment of the combined effects of low-symmetry ligand fields and dynamic Jahn–Teller coupling, the center of gravity of the ${}^3\text{T}_{2g}(\text{F})$ and ${}^3\text{T}_{1g}(\text{P}) (O_h)$ terms

will not, to first-order, depend on the magnitude of these effects. The energies of the spin-allowed transitions will, however, be strongly dependent on the magnitude of the axial field splitting of the ground term, and we use this fact to draw inferences regarding the geometry of the $[\text{V}(\text{OH}_2)_6]^{3+}$ cation in solution.

In Figure 6 is shown a schematic diagram depicting the increase in the energies of the spin-allowed transitions, which is expected as the twist angle decreases from 0° to -45° . This arises from the increasing stabilization of the ${}^3\text{A}_g (S_6)$ ground term. On the figure is given the magnitude of the trigonal field splitting of the ${}^3\text{T}_{1g}$ ground term for $\varphi = -21^\circ$ and -45° : 1940 and 2700 cm^{-1} , respectively. These values were determined by electronic Raman spectroscopy and are in excellent agreement with AOM calculations.^{19,20} The figure is of course oversimplified; the relative energies of the ${}^3\text{T}_{1g}(\text{F})$, ${}^3\text{T}_{2g}(\text{F})$, and ${}^3\text{T}_{1g}(\text{P})$ terms will shift slightly due to the off-diagonal trigonal field. Furthermore, a small increase in the Racah parameters is expected for the Rb[Ga:V]SH system on account of the tilt of the water molecules, which will also affect the transition energies.¹⁶ Nevertheless, AOM calculations, which we have performed using all 45 electronic basis functions,³⁹ suggest that such considerations are dwarfed by the change in the magnitude of the diagonal trigonal field splitting of the ground term. As φ decreases from 0° to -45° , a general increase in the transition energies of the ${}^3\text{T}_{1g}(\text{F}) \rightarrow {}^3\text{T}_{2g}(\text{F})$ and ${}^3\text{T}_{1g}(\text{F}) \rightarrow {}^3\text{T}_{1g}(\text{P}) (O_h)$ is expected on account of the stabilization of the ${}^3\text{A}_g (S_6)$ ground term, and this is borne out by the single-crystal absorption spectra presented in Figure 5.

Absorption spectra of solutions containing the vanadium(III) cation are well-known, and an excellent review article on vanadium(III) in aqueous solution has been provided by Roland Meier and co-workers.⁴⁰ The absorption spectra of vanadium(III) as a function of sulfate concentration have been particularly well characterized⁴⁰ as the $[\text{V}(\text{OH}_2)_6]^{3+}$, $[\text{V}(\text{OH}_2)_5(\text{SO}_4)]^+$, and $[\text{V}(\text{OH}_2)_4(\text{SO}_4)_2]^-$ complexes are thought to be present, in large concentrations, in the blood of ascidians.⁴¹ For the present study, care was taken to prepare a vanadium(III) solution free from anions such as sulfate and chloride because of their tendency to coordinate directly to vanadium(III).^{40,42} Triflate was chosen as the counteranion as it is both inert and a poor ligand. Furthermore, in the triflate salt $[\text{V}(\text{OH}_2)_6][\text{H}_5\text{O}_2](\text{CF}_3\text{SO}_3)_4$ the stereochemistry of the $[\text{V}(\text{OH}_2)_6]^{3+}$ cation has been shown to be close to all-horizontal D_{3d} by single-crystal neutron diffraction,¹³ a result at variance with the most energetically favored structure predicted by DFT calculations.⁴ The room temperature absorption spectrum of $\text{V}(\text{CF}_3\text{SO}_3)_3$ (0.2 M) dissolved in triflic acid (0.1 M) is shown in Figure 5, along with solid-state spectra. The peak maxima occur at very similar energies to those reported for the $[\text{V}(\text{OH}_2)_6]^{3+}$ cation

(37) Carver, G.; Tregenna-Piggott, P. L. W. Unpublished work.

(38) Bussière, G.; Beaulac, R.; Cardinal-David, B.; Reber, C. *Coord. Chem. Rev.* **2001**, 219–221, 509–543.

(39) LIGFIELD ver. 0.92, by Jesper Bendix 1998, Department of Chemistry, University of Copenhagen.

(40) Meier, R.; Boddin, M.; Mitzenheim, S.; Kanamori, K. *Met. Ions Biol. Syst.* **1995**, 31, 45–88.

(41) Frank, P.; Hodgson, K. O. *Inorg. Chem.* **2000**, 39, 6018–6027.

(42) Furman, S. C.; Garner, C. S. *J. Am. Chem. Soc.* **1950**, 72, 1785.

in perchlorate solutions of varying pH and ionic strength⁴³ suggesting no gross change in the electronic structure of the aqua ion as a consequence of exchange of triflate for perchlorate. The d–d transitions are not anomalously broad, and the band maxima are clearly closer in energy to those observed for Rb[Ga:V]SH ($\varphi \sim 0^\circ$) compared to GuVSH ($\varphi \sim -45^\circ$), suggesting that, in solution, the stereochemistry of the [V(OH₂)₆]³⁺ cation is closer to T_h than the all-horizontal D_{3d} geometry.

Good-quality high-field, high-frequency EPR spectra were obtained for RbVSH and GuVSH. The spectra for RbVSH have been presented previously, from which the ground-state spin-Hamiltonian parameters have been determined with excellent precision.¹⁶ As no EPR transitions attributable to a vanadium(III) species were observed for the [V(OH₂)₆]³⁺:trif sample, the EPR spectra of GuVSH do not assist in the main objective of the present study, and hence will be presented in a future publication, along with electronic Raman data. However, the reason why we were not able to observe an EPR spectrum for Rb[Ga:V]SH and [V(OH₂)₆]³⁺:trif must be addressed. For values of φ between 0° and -45° , the trigonal field lifts the degeneracy of the ³T_{1g} (O_h) ground term, leaving the ³A_g component lower lying.^{14,17} The 3-fold degeneracy is lifted to second-order by spin–orbit coupling, and the magnitude of the zero-field-splitting, D , is of the order $\sim(A\lambda)^2/\Delta$, for $A\lambda \ll \Delta$, where A is the expectation value of the \hat{L}_z operator.²⁹ For RbVSH, $D = 4.906(4) \text{ cm}^{-1}$,¹⁶ whereas for GuVSH, $D = 3.73(5) \text{ cm}^{-1}$,²⁰ the reduction in D being consistent with the increase in the magnitude of the trigonal field. For values of φ close to zero, D and $dD/d\varphi$ are large because of the $\sin 2\varphi$ dependence of the trigonal field (eq 1). A relatively small distribution in the value of φ would then give rise to a large distribution in the range of D values, such that inhomogeneous broadening would render the EPR spectrum undetectable. We believe that it is for this reason that we were unable to observe an EPR spectrum for [V(OH₂)₆]³⁺:trif. Using a similar approach as that applied to calculate the ground-state g values of [Ru(OH₂)₆]³⁺, we have calculated the D vs φ relation, from which EPR band profiles for [V(OH₂)₆]³⁺ have been calculated, for differing degrees of inhomogeneity. If the values of φ were distributed between -35° and -45° for [V(OH₂)₆]³⁺:trif, as we have inferred for [Ru(OH₂)₆]³⁺:trif, the inhomogeneous broadening

(43) See Table 1 of ref 40 for a compilation of UV–vis parameters for [V(OH₂)₆]³⁺ in a variety of acidic aqueous electrolytes.

would not be so severe; we would have expected to observe an EPR spectrum. The inability to observe an EPR spectrum for Rb[Ga:V]SH, down to temperatures of $\sim 5 \text{ K}$, may also be a consequence of efficient spin–lattice relaxation.

5. Summary

In this work, spectroscopic data have been presented and analyzed for the [Ru(OH₂)₆]³⁺ and [V(OH₂)₆]³⁺ cations, both in the solid state and in aqueous solution. The EPR study of [Ru(OH₂)₆]³⁺ provides strong evidence that, in solution, the aqua ion is localized in the all-horizontal D_{3d} geometry. Absorption spectra for the [V(OH₂)₆]³⁺ cation are consistent with the aqua ion adopting a geometry close to T_h symmetry. This inference is tentative, however, as attempts to determine the ground-state electronic structure directly by high-field multifrequency EPR were not successful.

Our conclusions are consistent with the most energetically favored structures of the [Ru(OH₂)₆]³⁺ and [V(OH₂)₆]³⁺ cations predicted by ab initio calculations^{3,4}—bravo. This work should bring cheer to quantum chemists who model chemical reactions in aqueous media.⁵ However, we recommend that caution be applied when rationalizing solid-state phenomena on the basis of the results of the same calculations. It is curious that the [V(OH₂)₆]³⁺ cation in dilute triflic acid seems to adopt a stereochemistry close to T_h but, in the salt formed from the saturated solution, the structure is close to all-horizontal D_{3d} . Furthermore, in the following paper, it shall be shown that the value of φ in the cesium β alums of formula Cs[M^{III}(OD₂)₆](SO₄)₂·6D₂O is anomalously negative for both the Ru(III) and V(III) cations,¹² suggesting that, in the solid state, both these aqua ions exhibit a tendency to distort towards the all-horizontal D_{3d} structure. The ongoing challenge for quantum chemists is to tackle molecules of ever-increasing size and complexity. As far as the aqua ions are concerned, it would be interesting to calculate the energy of the complexes along the T_h – S_6 – D_{3d} potential energy surface when the second coordination sphere is included. The value of φ , corresponding to the configuration of minimum energy, may well be dependent upon the strength of the hydrogen bonds, emanating from the aqua ion.

Acknowledgment. We are very grateful to Margret Biner for providing us with a sample of [Ru(OH₂)₆](tos)₂. This work was funded by the Swiss National Science Foundation.

IC025962G